# STATISTICS OF OPTICAL AND GEOMETRICAL PROPERTIES OF CIRRUS CLOUD OVER TIBETAN PLATEAU MEASURED BY LIDAR AND RADIOSONDE

**Guangyao Dai[1, 2*], Songhua Wu[1, 3], Xiaoquan Song[1, 3], Xiaochun Zhai[1]**

[1]*Ocean University of China: Ocean Remote Sensing Institute, Qingdao, China, *dai@tropos.de*
[2]*Leibniz Institute for Tropospheric Research, Leipzig, Germany*
[3]*Laboratory for Regional Oceanography and Numerical Modeling, Qingdao National Laboratory for Marine Science and Technology, Qingdao, China*

## ABSTRACT

Cirrus clouds affect the energy budget and hydrological cycle of the earth's atmosphere. The Tibetan Plateau (TP) plays a significant role in the global and regional climate. Optical and geometrical properties of cirrus clouds in the TP were measured in July-August 2014 by lidar and radiosonde. The statistics and temperature dependences of the corresponding properties are analyzed. The cirrus cloud formations are discussed with respect to temperature deviation and dynamic processes.

## 1 INTRODUCTION

Cirrus clouds play a significant role in the energy budget and the hydrological cycle of the earth atmosphere. Cirrus affects the climate via two opposite effects; an infrared greenhouse effect and a solar albedo effect [1]. Since the significant role the cirrus plays, a clear understanding of their optical and geometrical properties is highly essential for climate modeling studies.

The TP is a vast elevated plateau in the middle of the Eurasian continent with averaged elevation 4.5 km above mean sea level (a.m.s.l.), and it has an important role in the global and regional climate system. The TP lies at a critical and sensitive junction of four climatic systems: the Westerlies, the East Asian monsoon, the Siberian cold polar airflow and the Indian monsoon [2]. During July and August 2014, atmospheric measurements were carried out in the TP for the first time to our knowledge using a ground-based high power depolarization and Raman lidar.

## 2 INSTRUMENT AND EXPERIMENT

A three-wavelength combined elastic-backscatter Raman lidar, water vapor, cloud and aerosol lidar (WACAL) is used to perform continuous measurements of cirrus clouds. The vertical resolution of the signal is equal to 3.75 m and the temporal resolution is 30s. In our study, the radiosonde of GTS1 type is utilized. The radiosonde provides temperature with accuracy of $\pm 0.2\,℃$, relative humidity accuracy of $\pm 5\%$ and pressure accuracy of $\pm 1\,\mathrm{hPa}$.

During July and August 2014, we conducted the third TP Experiment of Atmospheric Sciences (TIPEX III) by using WACAL in Naqu (31.48 °N, 92.06°E, 4508 m). To investigate the temperature dependence of the optical and geometrical

properties of cirrus, simultaneous observations by WACAL and radiosonde are combined. Consequently, only the concurrent measurements by WACAL and radiosonde at nighttime were taken into account and the optical and geometrical characteristics as well as the temperature of cirrus clouds were analyzed.

## 3 METHODOLOGY

We determined the linear volume depolarization ratios (LVDR) using the "±45°-calibration" [3]. The extinction coefficients are calculated by the Fernald method but they are corrected by removing the multiple-scattering effect. Also, the WACAL is capable of detecting the cloud base height and even the cloud top height if the clouds can be penetrated by laser. To determine the cloud height, an algorithm that combines "differential zero-crossing algorithm" and "threshold algorithm" is used.

## 4 RESULTS AND DISCUSSION

During the TIPEX III, 21 measurements of cirrus clouds were performed. The occurrence frequency of the cirrus clouds is about 20.75%.

### 4.1 Geometrical characteristics

In Figure 1, we present the cirrus structure and the vertical distribution of the occurrence frequency of cirrus base/top heights (CBH/CTH) measured during the TIPEX III. The maximum frequencies of the CBH and CTH are 33.33% at a height of 6-7 km above ground level (AGL) and 23.80% at a height of 7-8 km AGL, respectively. The CBH ranges from 4 to 12 km AGL, with a mean value of $7.4 \pm 2.0$ km. The CTH ranges from 5 to 13 km AGL, with a mean value of $8.5 \pm 2.0$ km.

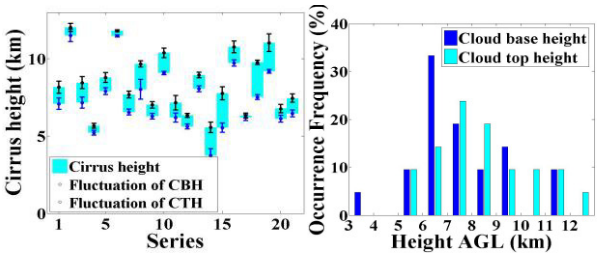


*Figure 1: (a) Cirrus structure and (b) the histogram of cloud base/top heights.*

Histograms of cirrus cloud middle height and mean temperature are presented in Fig. 2. Cirrus clouds are generally observed in the TP from 4 to 12 km AGL, with mid-cloud temperatures ranging from -79.7 to -26.0 °C, and have a mean temperature of $-46.1 \pm 15.5$ °C. There were two peaks of occurrence frequencies of the cirrus middle height, including 28.57% at 6-7 km and 19.05% at 8-9 km AGL, respectively. From Fig. 2 (b), the maximum frequency of the cirrus middle temperature is 38.10% between -40 and -30 °C.

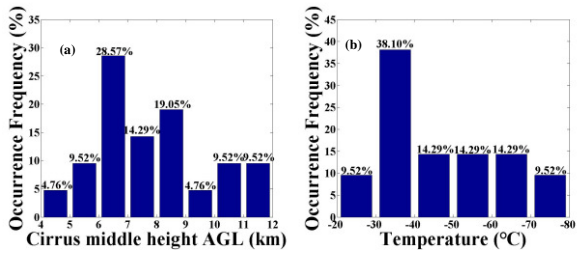


*Figure 2: (a) Cirrus middle height occurrence frequency and (b) temperature occurrence frequency.*

From Fig. 3, the cloud thickness ranges from 0.12 to 2.26 km, with 81% of the case studies have thickness between 0.5 and 2 km. The cirrus thickness distribution has a skewed normal distribution. The maximum frequency of the cirrus thickness is 38.10% between 0.5 and 1 km while the minimum frequency is 4.76% between 2 and 2.5 km.

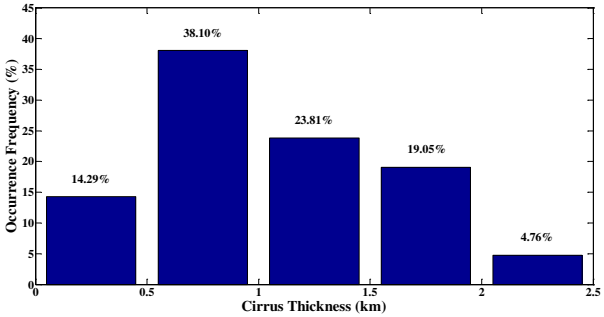


*Figure 3: Cirrus cloud thickness*

## 4.2 Optical properties

In Fig. 4, the LVDR, the extinction coefficient and the corresponding statistical uncertainties are presented. From this figure, the LVDR ranges from 0.3 to 0.55, while the extinction coefficient ranges from $10^{-5}$ $m^{-1}$ to 0.005 $m^{-1}$. For further investigation, we present the distribution and histogram of the cirrus clouds optical depth in Fig. 5. The optical depth of all the cirrus clouds is between 0.01 and 3. It is found that 14.29% of cirrus clouds are sub-visible (optical depth<0.03), 66.67% are optically thin (0.03<optical depth<0.3) and 19.04% are opaque (optical depth>0.3).

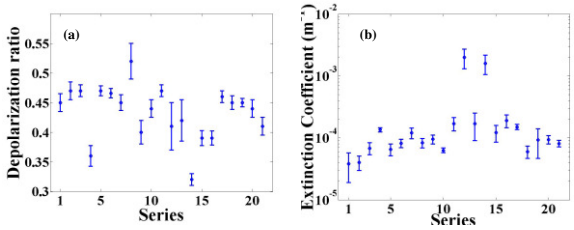


*Figure 4: (a) LVDR and (b) Extinction coefficient and statistical uncertainties*

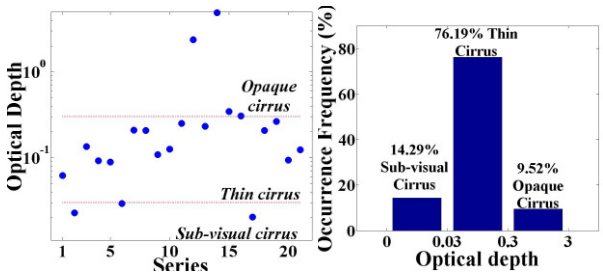


*Figure 5: (a) Distribution of optical depth and the classification of all the cirrus clouds, (b) Occurrence frequency of different types of cirrus clouds.*

## 4.3 Temperature dependence of optical properties

Figure 6 shows the LVDR dependences on temperature and cirrus middle height. The LVDR of cirrus varies from 0.3 to 0.55. With the increase of the temperature, the values of the LVDR are gradually reduced. We propose that with the decrease of the temperature and the increase of cirrus middle height, the irregular ice types with larger size and greater distortion are formed, which result in the increase of LVDR of the cirrus clouds. According to Fig. 6, it can be seen that the LVDR with higher temperature and lower altitude is much more sensitive to the ambient temperature.

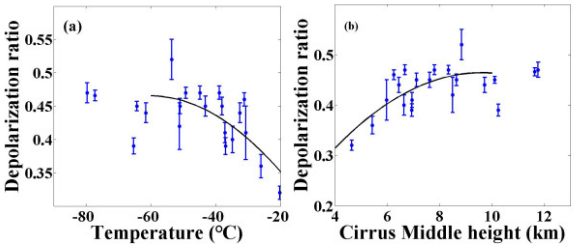


*Figure 6: (a) Scatter diagram of LVDR and temperature, (b) Scatter diagram of LVDR and cirrus middle height.*

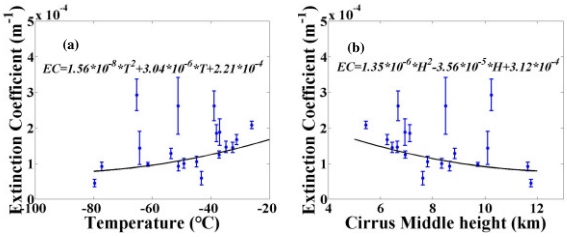


*Figure 7: (a) Scatter diagram of extinction coefficient and temperature, (b) Scatter diagram of extinction coefficient and cirrus middle height.*

Figure 7 shows the extinction coefficient

dependences on temperature and cirrus middle height. From Fig. 7, the mean extinction coefficient decreases with decreasing temperature. Although the cirrus radiative properties depend on cloud microphysics, it is the ambient temperature that governs the radiative transfer since it dominates the cloud microphysics. Due to the stability of the larger cirrus particle radius in the extremely low temperature, the temperature sensitivity of the extinction coefficient is found gradually weak with the decreasing temperature. Consequently, temperature has a bigger impact on the extinction coefficient for warmer and lower cirrus.

Figure 8 presents the temperature anomalies during July and August 2014 over Naqu. The warm color corresponds to the positive deviation while the cool color corresponds to negative deviation. Moreover, the CBH and CTH are also plotted in Fig. 8. The lidar observations can be separated in six stages: 10 to 11 July, 18 to 22 July and 31 July to 08 August for the cirrus appearances stages and 12 to 17 July, 23 to 30 July and 09 to 16 August for the cirrus blank stages. During the 3 cirrus appearances stages, the temperatures were higher than the average value, which indicates that the formation of the cirrus clouds may be related to the local ground heating of TP. The cold perturbations were found at a height of about 12 km AGL. During the 3 cirrus blank stages, warmer air mass existed at a height of above 12 km AGL. The tropospheric temperatures with the presence of cirrus were about 5 °C higher than those when no cirrus clouds existed. Consequently, the Rossby waves can best be recognized at a height of 16.5 km a.m.s.l. in the tropospheric layer and with a duration cycle of about 10 days. To conclude, the formation of cirrus clouds over TP is dominated by the Rossby wave and deep convective activity caused by local ground heating.

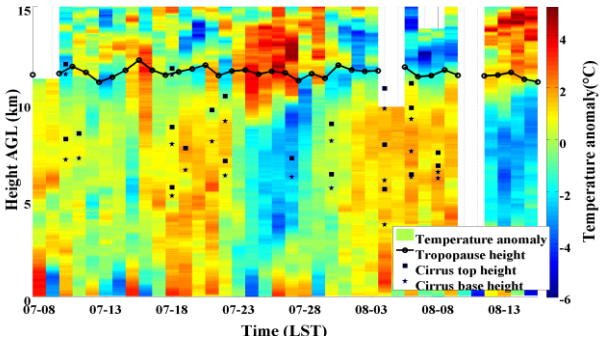


*Figure 8: Temperature anomalies during July and August 2014.*

## 5 SUMMARY AND CONCLUSION

This study provides an analysis of the geometrical and temperature characteristics as well as the optical properties of cirrus clouds over TP. The results show that cirrus clouds are occurring between 8.5 to 16.5 km a.m.s.l., with temperatures ranging from -79.7 to -26.0 °C . The cloud thickness ranges from 0.12 to 2.26 km with a mean thickness of $1.07 \pm 0.56$ km. The LVDR differs from 0.3 to 0.55, with a mean value of 0.43 $\pm 0.045$.

The cirrus clouds are classified as sub-visible cirrus (14.29%), optically thin cirrus (66.67%) and opaque cirrus (19.04%) judging by the optical depth.

From the temperature anomaly from July to August in 2014, the formation of cirrus clouds has apparent relationship with the dynamic processes of Rossby wave and deep convective activity over TP.

## ACKNOWLEDGEMENTS

This work was supported by the National Natural Science Foundation of China (NSFC) under grant 41375016 and 91337103, by the China Special Fund for Research in the Public Interest under grant GYHY201406001.

## References

[1] Giannakaki, E., Balis, D., Amiridis, V., and Kazadzis, S., 2007: Optical and geometrical characteristics of cirrus clouds over a Southern European lidar station, *Atmos. Chem. and Phys.*, **7**(21), 5519-5530.

[2] Wu, S., Dai, G., Song, X., Liu, B., and Liu, L., 2016: Observations of water vapor mixing ratio profile and flux in the TP based on the lidar technique, *Atmos. Meas. Tech.*, **9**(3), 1399-1413.

[3] Freudenthaler, V., Esselborn, M., Wiegner, M., Heese, B., Tesche, M., Ansmann, A., Müller, D., Althausen, D., Wirth, M., and Fix, A., 2009: linear volume depolarization ratios profiling at several wavelengths in pure Saharan dust during SAMUM 2006, *Tellus B*, **61**(1), 165-179.